symmetry

MDPI

Article

Disdrometer Performance Optimization for Use in Urban Settings Based on the Parameters that Affect the Measurements

Ferran Mocholí Belenguer [1,*], Antonio Martínez-Millana [2], Antonio Mocholí Salcedo [3], Víctor Milián Sánchez [4] and María Josefa Palomo Anaya [4]

1 Traffic Control Systems Group, ITACA Institute, Universitat Politècnica de València, 46022 Valencia, Spain
2 SABIEN Group, ITACA Institute, Universitat Politècnica de València, 46022 Valencia, Spain; anmarmil@itaca.upv.es
3 Department of Electronic Engineering, ITACA Institute, Universitat Politècnica de València, 46022 Valencia, Spain; amocholi@eln.upv.es
4 Chemical and Nuclear Engineering Department, Institute of Industrial, Radiological and Environmental Safety, Universitat Politècnica de València, 46022 Valencia, Spain; vicmisan@iqn.upv.es (V.M.S.); mpalomo@iqn.upv.es (M.J.P.A.)
* Correspondence: fermocbe@upv.es; Tel.: +34-610833056

Received: 15 November 2019; Accepted: 13 February 2020; Published: 20 February 2020

Abstract: There are currently different types of commercial optical disdrometers to measure the rainfall intensity, of which many are commonly used for monitoring road conditions. Having information about the amount of rain, the composition of the precipitation particles and visibility are essential to avoid accidents, which requires intelligent systems that warn drivers and redirect traffic. However, few studies related to Intelligent Transport Systems (ITS) have been performed regarding why these devices are not optimized for this type of applications. Therefore, this paper analyzes and evaluates the operating mode of these equipment through their theoretical model, which will allow the design of prototypes of disdrometers with different characteristics. In addition, this model will be implemented in a simulation program, through which an exhaustive study analyzing how the type of precipitation and its intensity affect the measures provided by the model will be conducted. In this way, the results will help optimize its operation to be thus used in urban settings, which will allow obtaining more accurate real-time information, better traffic management, and a reduction in the number of accidents.

Keywords: disdrometer; precipitation; rain; safety; traffic

1. Introduction

For a long time, many series of rainfall records have been made throughout the world [1,2]. These records, which are expressed in mm or kg/m^2 and collected during a certain time period, have been useful for meteorology and climatology and are of special interest to many sectors such as hydrology, agriculture, or vehicle traffic management systems [3]. However, although recording the amounts of precipitation of liquids and solids constitutes a knowledge base in several fields of study, the precipitation intensity (PI) has become a variable of the same importance at present.

The precipitation intensity is defined by the World Meteorological Organization as the amount of precipitation collected per unit time, and it is widely known that the rainfall and snowfall intensity information is extremely relevant in cases of severe weather [4,5]. In fact, high precipitation intensities in the form of liquid or solid directly affect transport, since roads and other infrastructure can be blocked in cases of insufficient drainage and runoff [6]. Moreover, the probability of having an accident while it rains or snows is greater than when it does not [7], which is mainly due to the lack of visibility.

Hence, appropriate short-term forecasts could reduce these risks and allow the sending of warnings to drivers to take precautions or avoid certain routes. This is the reason why many types of instruments and measuring techniques have been developed and are in operation today. In this way, there are different types of instrument that measure precipitation micro-physical parameters and divide into remote sensing and in-situ [8].

Depending on how they work, all types of rain gauges can be divided into two large groups:

1. Catching instruments.
2. Non-catching instruments.

The first type catches the precipitation through a well-defined hole size and measures the equivalent mass or volume of water that has accumulated in a given time interval. In this sense, the precipitation intensity is retrieved from the amount of precipitation. On the contrary, the non-catching instruments calculate the precipitation intensity by mathematically integrating all particles transiting through a cross section in a given time. Optical, acoustic, and electromagnetic rain sensors are typical examples of this group.

Nevertheless, although many calibration practices have been developed, especially for the rain gauges of the first group, there is currently no standard or accepted calibration reference for any type of rain gauge. Therefore, CIMO-XIII (The Thirteenth Session of the Commission for Instruments and Methods of Observation) adopted the measurement range and uncertainties related to the precipitation intensity recommended by an expert group of researchers who published that information in the Guide to Instruments and Methods of Observation of the World Meteorological Organization [9]. These data are shown in Table 1.

Table 1. Uncertainties adopted by CIMO-XIII.

Full range	0.02–2000 mm·h^{-1}
Rainfall threshold detected	0.02–0.2 mm·h^{-1}
Output averaging time	One minute
Uncertainty required in the measurement:	
0.2–2 mm·h^{-1}	0.1 mm·h^{-1}
2–2000 mm·h^{-1}	5%

Accordingly, as these are commonly used on roads to warn and therefore prevent accidents and there are no studies with the purpose of optimizing their operation for these applications, we think that there is clearly a need to have an adaptive and optimized system capable of measuring the intensity of precipitation meticulously depending on the type of rain, wind, and other parameters. In this way, these devices could be adapted according to the boundary conditions, always providing the most accurate measurements. In addition, minimum and specific requirements could be established so that they could be installed and used in ITS applications. These requirements would be as follows:

1. It should be a simple, low-cost system implemented with commercial materials.
2. It should use optoelectronic systems, since the analysis performed by many authors suggests that these systems provide better results [10,11].
3. It should be capable of operating both at fixed stations in the road network and onboard a vehicle to provide information to the driver and activate the fog lights or windscreen wipers when required.

There are some disdrometer models such as Parisivel that could meet these specifications, but Grossklaus et al. [10] presented a model of a disdrometer that satisfied these requirements in a better way. Indeed, a few years later, the company Eigenbrodt manufactured the optical disc ODM470 by following the specifications indicated by them. Thus, this manuscript will theoretically analyze the operation of this equipment and evaluate the effects of a series of parameters on it,

such as the precipitation intensity, drop size distribution, period sampling method, estimation method, measurement time, wind speed, type of converter, and many others. For this, a program exclusively designed by our work group has been implemented, which enables to simulate the behavior of the equipment by varying its parameters.

2. Materials and Methods

2.1. Operating Principle

The principle of operation of the aforementioned disdrometer is the slight decrease in light intensity when the raindrops pass through a cylindrical sensitive volume of length L and diameter D [12]. At one end of the cylinder, there is a light source, which is usually an IR LED diode with a control system that enables the diode to maintain its level of illumination constant. At the other end, there is a photodetector, which is a photodiode with a signal conditioning circuit in most cases. To achieve a homogeneously illuminated sensitive volume, a suitable optical lens system composed of a collimator and Fresnell lens is also required. This scheme is shown in Figure 1, which can simultaneously measure the size and flight time of the droplets through the sensitive volume.

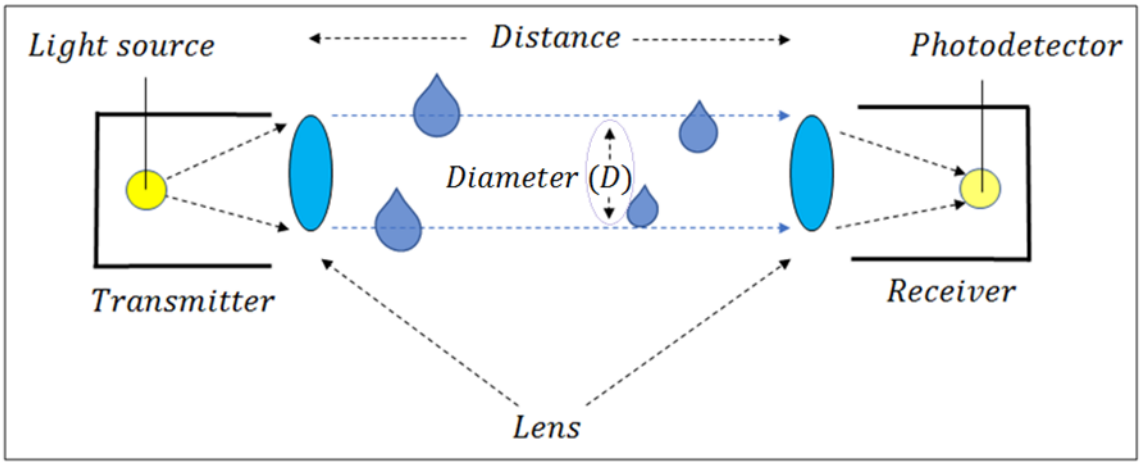

Figure 1. Implementation of an optical disdrometer.

During a precipitation event, important fluctuations will be observed in the photodetector whenever a particle interferes with the light beam emitted by the LED. The amplitude of these fluctuations depends on the size of the particles, while the duration of the fluctuations is depending on raindrop fall speed. Moreover, the number of fluctuations is proportional to the number of particles that pass between the LED and the photodetector. The only constraints that may occur are the system dependence on the frequency of sampling of the signal, and the resolution in the illumination level measurement. However, the operating ranges of different instruments and our analysis will demonstrate that these constraints will not be an inconvenience that limits the system operation.

2.2. Drop Size Measurement

If there is no drop inside the sensitive volume, the illumination that reaches the photodetector will induce an output signal, which will be taken as a reference. When raining, each drop through the sensitive volume produces a reduction of light received by the photodetector, and the corresponding signal is proportional to the quotient between the area of the section-line of the drop and the area of the section-line of the sensitive volume. Hence, the range of amplitudes of the signal may vary between 0 and the amplitude of the reference signal. Depending on the type of photodetector and signal conditioning, the magnitude to be measured can be a voltage, a current intensity, or a frequency, which

also conditions the type of microcontroller to manage the operation of the disdrometer. Nevertheless, the maximum sensor response will occur for a particle of at least diameter D as shown in Figure 1.

The tests performed by different authors [10] show that the homogeneity and isotropy of light in the sensitive volume are essential for the correct interpretation of the data. Unfortunately, most lighting sources have some anisotropy and inhomogeneities. Thus, inhomogeneities along the length of the optical volume, such as those due to the divergence of light, must be minimized. In our model, we consider the ideal case of a perfectly collimated source, so the errors estimated must be improved to consider this effect.

As indicated, the slight decrease in light signal E is proportional to the quotient between the area of the section-line of the drop and the area of the section-line of the sensitive volume. Moreover, the optical volume sensitivity can be accurately calibrated using metal spheres of different diameters. Figure 2 shows the relative theoretical attenuation as a function of the quotient between the droplet diameter d and diameter D of the sensitive volume.

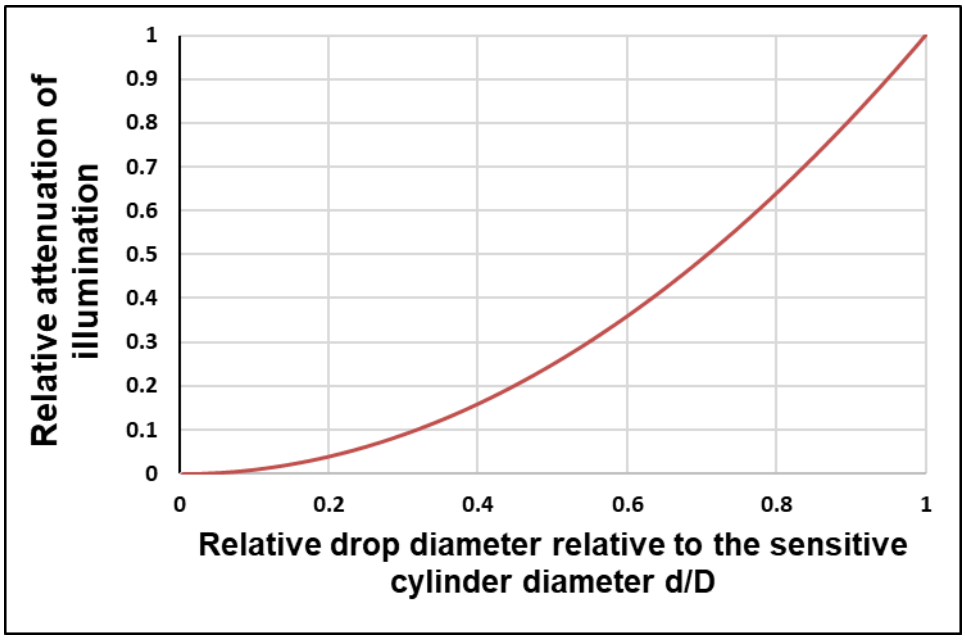

Figure 2. Theoretical relationship between light attenuation and the droplet diameter.

2.3. Signal Duration Measurement

The drops that penetrate the sensitive volume are detected as soon as the signal variation of the photodetector exceeds a defined threshold. Thus, the microcontroller will continuously monitor the value of this signal and indicate the instants of entry and exit of the drop in the measurement volume.

The precision in the measurement of these times only depends on the maximum measurement speed of the system and the minimum variation of the signal that can be detected. Depending on the clock frequency, hardware and implemented programming, we will finally be able to obtain a value of the time between measures (ΔT_{sam}), which represents the maximum delay in the detection of a drop that is entering or leaving the sensitive volume and consequently the determination of the signal duration. In other words, the output time minus input time in the volume has an error of $\pm\Delta T_{sam}$. However, this error can be considered unsystematic.

2.4. Data Processing

As long as the drops that impact tangentially on the sensitive volume are ignored, the errors in the diameter estimation will be conditioned by the characteristics of the measuring instrument.

The response of the photodetectors is established by the surface covered by each drop; the cause of its variation is linked to the square of the diameter of those drops as shown in Figure 1.

Meanwhile, conventional digital systems work with A/D converters, whose resolution is a function of their number of bits (n_{bits}), which results in $2^{n_{bits}}$ measurement levels. Then, the surface resolution of the detector is given by $\frac{(\pi D^2)}{2^{2+n_{bits}}}$. Most studies propose an 8-bit converter, but we will compare the results obtained when using 8-bit and 10-bit converters.

Over time, some techniques have been proposed to estimate the precipitation intensity from the information provided by the sensors, but in all cases, the drops are classified according to their size. The two most commonly used techniques are presented below: time technique and counting technique.

2.5. Time Technique

It is known that during sampling time T, a certain number of drops have fallen through the sensitive volume with a cumulative transition time of $\sum t_i$. Illingworth and Stevens [13] showed that for each droplet size, the fraction of time $\frac{\sum t_i}{T}$ indicated the number of drops directly within sensitive volume V. However, this relation is only valid if there are many raindrops evenly distributed in space and if sampling time T is large compared to the time of the droplet transition. In this case, the number density of raindrops is expressed as

$$N_{(size)} = \frac{\sum t_{i(size)}}{V \cdot T} \tag{1}$$

This calculation does not depend on the wind speed because an increase in wind speed increases the number of drops that reach the disdrometer in the same proportion when the transit time decreases. Meanwhile, the number density of drops is defined by considering only those droplets whose centers are within the volume. Thus, the time of transition of the raindrops that reach the sensitive volume is defined as the time that passes from when the center of a drop enters the sensitive volume to when it leaves this volume. Then, the total duration t_s of the signal must be converted to transition time t from the center of a drop as

$$t = t_s \frac{D}{d + D} \tag{2}$$

where d is the diameter of the drop and D is the diameter of the sensitive volume.

2.6. Counting Technique

The droplet size spectra can also be determined by using the number of drops that penetrate the sensitive volume. By knowing local wind speed U and assuming that the vertical velocity of the raindrops is V_{fall}, we can calculate the effective velocities of the drops. Length L and diameter D of the sensitive volume define the area of the side view $(L \cdot D)$ of this volume. Multiplying this area by the effective rate of passage of the droplets of a certain size gives an imaginary amount of air V_L that passes through the disdrometer during sampling time T. This volume contains all droplets of a given size that reach the sensitive volume of the disdrometer within a sampling period

$$V_{L(size)} = L \cdot D \cdot T \sqrt{U^2 + \left[V_{fall(size)}\right]^2} \tag{3}$$

The number density of drops of identical size is obtained as the quotient of the total number of drops detected divided by volume V_L

$$N_{(size)} = \frac{A_{size}}{V_L} \tag{4}$$

The counting technique requires more assumptions than the time technique. For example, in this technique, the local wind speed must be known. Nevertheless, the terminal fall rate of raindrops can be estimated by the formula [14]

$$V_{fall}(d) = 17.67 \cdot d^{0.67} \tag{5}$$

where d is the diameter of the drop in centimeters, and the resulting drop rate is obtained in m/s. This parameterization has been chosen against other options because it is the most novel. However, the results do not significantly differ from those offered by other authors [15], so any of them could be used.

To study the advantages and disadvantages of the two techniques, numerical simulations of measurements with the same precipitation model were performed, and the results are shown below.

2.7. Precipitation Intensity Calculation

The precipitation intensity (PI) can be obtained from the droplet size spectrum by applying

$$PI = \sum_{size=1}^{N_{size}} N_{size} \cdot V_{fall(size)} \cdot M_{drop(size)} \quad (6)$$

where $M_{drop(size)}$ is the mean mass of the droplets that are classified within the same size. The precipitation intensity has units of $\frac{kg}{m^2 s}$ if N_{size} is given in m^{-3}, $V_{fall(size)}$ is measured in $\frac{m}{s}$, and $M_{drop(size)}$ is measured in kg. The value of $M_{drop(size)}$ can be determined by assuming a spherical shape of the drops. Thus, it is quite simple to calculate the mass of a spherical drop from its straight section. However, large and real droplets have an oblong shape due to their aerodynamic properties. This effect has been analyzed [13], which verifies that the vertical cross-sectional area of a drop decreases when it deforms (elongates), which starts approximately for a 1.5 mm drop diameter. This effect causes a lower estimate of the drop volume. Figure 3 shows similar results to those obtained by Pruppacher and Pitter [16].

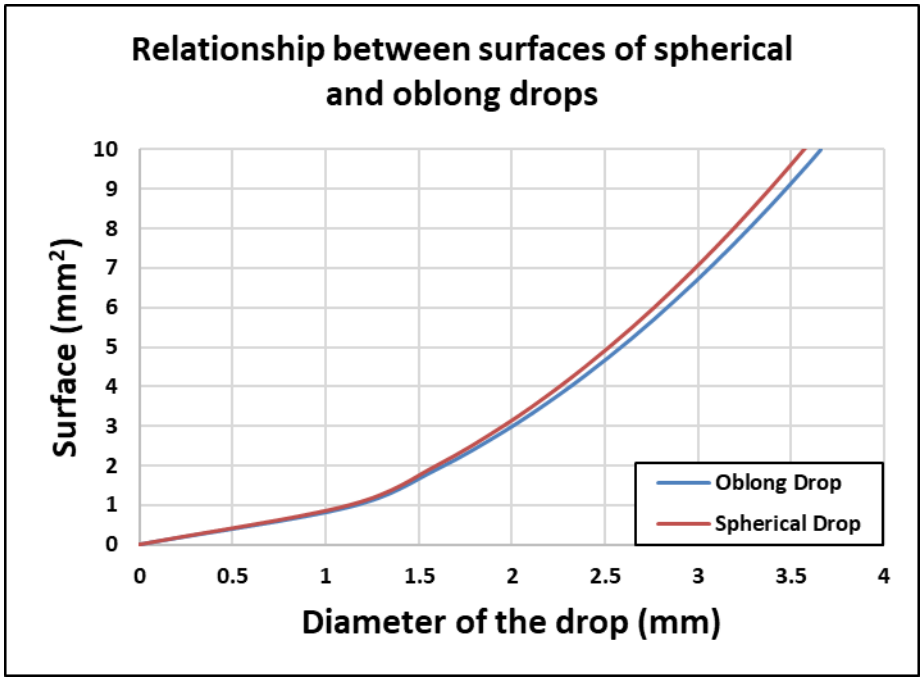

Figure 3. Effect of the drop oblateness.

Rain can wet the outer lenses of the disdrometer due to splashes of large drops. The droplets that wet the lens will cause electronic signals that will be characterized by their small amplitudes and long durations. This type of disturbance can cause an overestimation of the number density of small drops.

To prevent this effect, we propose to perform a special filtration. Using this filter, those signals whose duration exceeds a defined time period are eliminated. This threshold is set as the maximum possible duration of the signal generated by a drop of the detected size with respect to its terminal

velocity and applying a time factor of 1.5. The filter time is called T_{max} and is adjustable in our model, although it will not act in any case, since the aforementioned splashes are not simulated.

2.8. Edge Effects

In the work of Grossklaus et al. [17–19] a series of phenomena that affect rainfall estimation are presented, which are called the edge effects. One of these main effects is the equivocal detection of water drops, which results in the cases detailed below, but there are other edge effects such as those due to drops just grazing the sensitive volume which also systematically influence the disdrometer measurements. However, as all of them can be described statistically, a correction is possible. Hence, all of these effects and the techniques proposed for their correction are considered and implemented in our model.

In normal precipitation, drops of a wide range of sizes may be mixed. Therefore, the sensitive volume of the disdrometer should be sufficiently large to provide a reasonable probability of correctly measuring large droplets, which significantly contribute to the rainfall intensity. However, only the amount of shadow produced is measured, regardless of whether it is caused by one or more drops on the sensitive volume at any given time. These coincidences have two effects:

1. Two small drops can be detected as a larger drop. In this case, a larger amount of water than the one that actually contains the two smaller drops is detected.
2. The time of the transition detected as a consequence of the coincidence of two drops is larger than that corresponding to a drop of larger diameter, which simulates a greater probability of large drops and consequently an exaggerated contribution to the determination of the precipitation intensity.

Nevertheless, as these effects have a systematic influence on the measurement performed by the disdrometer, a statistical analysis enables to correct these effects. This error variance of the disdrometer measurements is estimated, considering the following effects that contribute to this variance [10]:

1. "The iterative procedure to compensate for the fringe effects is based on the assumption that these effects occur according to their mean statistics. The Monte Carlo studies are used to quantify the portion of the total error variance produced by the random occurrence of the fringe effects. This will be referred to in the following as (fringe effects).
2. The Monte Carlo simulations also consider the inhomogeneity and anisotropy of the sensitive volume. The variance that is caused by this effect is therefore included in the variance obtained from the Monte Carlo model.
3. The total error variance also includes a sampling error due to the fact that even at a constant rainfall the number of drops penetrating the sensitive volume varies from one measurement to another. This sampling error has not been considered in the Monte Carlo simulations. This variance that is only caused by the sampling error will be called. The value of was determined analytically".

2.9. Numerical Model

To quantify the edge effects, the measurements made by the disdrometer were numerically modeled. Hence, our research team (Group of Traffic Control System, ITACA Institute, Universitat Politècnica de València, Spain) designed a simulation program in VisualBasic. This program enables to optimize the starting geometric data, such as the diameter or length of the sensitive volume. The maximum and minimum values of the droplet size to be measured and the resolution in the measurement of the diameters (number of bits of the A/D converter) are also adjustable.

Next, a series of data on the type of precipitation, such as the wind speed and precipitation intensity, must be provided. Since the droplet size distribution follows rules that depend on where the test is performed, it was decided to use a gamma function as law. This distribution was chosen because it was the same used by Grossklaus et al. [17–19] and Marshall and Palmer [20] in their studies, which has proven to describe satisfactorily the concentrations of the smaller droplets. From this gamma

function, the parameters N_0 and μ must be entered, and the system calculates the value of γ for the indicated precipitation intensity. To facilitate its use, two distributions of standard precipitation droplets—namely, stratiform and convective—are placed. In this way, although many studies analyzed this gamma distribution [20–25], in our study, the parameters used to describe these spectra were taken from Ulbrich [21,22], which can be seen in Table 2.

Table 2. Drop surface distribution parameters.

Type of Precipitation	N_0 ($m^{-3}cm^{-1-\mu}$)	μ
Convective	7.54×10^6	1.63
Stratified	1.96×10^5	0.18

The next information to be supplied is the sampling time, time resolution and number of tests to perform. Finally, to correct possible edge effects, the value of T_{max} must also be provided and indicate whether the effects of an excess of time of presence of the drop and the effect of the size of the drop on the duration time of each signal should be compensated.

With all of this information, the program begins by calculating the drop distribution that corresponds to the indicated intensity and type of precipitation. The distribution of droplet size in natural rainfall is irregular. However, simple mathematical formulas are often recommended to describe these distributions. According to Marshall and Palmer [20], the normally used parameterization only requires two parameters

$$N(d, \Delta d) = N_0 \cdot e^{-\Lambda d} \tag{7}$$

where $N(d, \Delta d)$ is the concentration of droplets with diameters between d and Δd; N_0 is the cut-off point for parameter $d = 0$ mm; and Λ is the slope parameter. Nevertheless, this formulation does not represent a maximum of medium-sized rain drops as occurs in actual measurements. Therefore, the distributions of three parameters have been introduced (gamma distributions use a third parameter μ that defines the shape of a drop size distribution). In this way, Figure 4 represents the distribution of the size of drops for different types of precipitation, which are characterized by N_0 and μ, as stated in different works such as that of Ulbrich or Martin [10].

Ulbrich [21,22] shows that there is a definite relationship between parameters N_0 and μ. This relationship is given by

$$N_0 = 6.0 \times 10^4 \cdot e^{3.2 \cdot \mu} \tag{8}$$

Therefore, the gamma distribution can be described using only two parameters.

With this information, a drop distribution is assigned according to the size to obtain the PI specified in the data. By applying an iterative procedure on the value of the gamma function, we determine the number of drops that correspond to the central value diameter of each existing band between the minimum and maximum drop values. At the beginning of each iteration, the analytical model is initialized with a drop size distribution that is assumed to be true. Then, the measurement of the simulated spectrum of the disdrometer is compared with its actual measurement. The convergence is achieved if these spectra differ by less than 2%. A new iteration starts again after the initial spectrum is modified according to the results of the previous iteration. In most cases, the convergence should be achieved in less than three iterations. The best results are achieved by using the same drop size distribution measured as the spectrum of the first iteration.

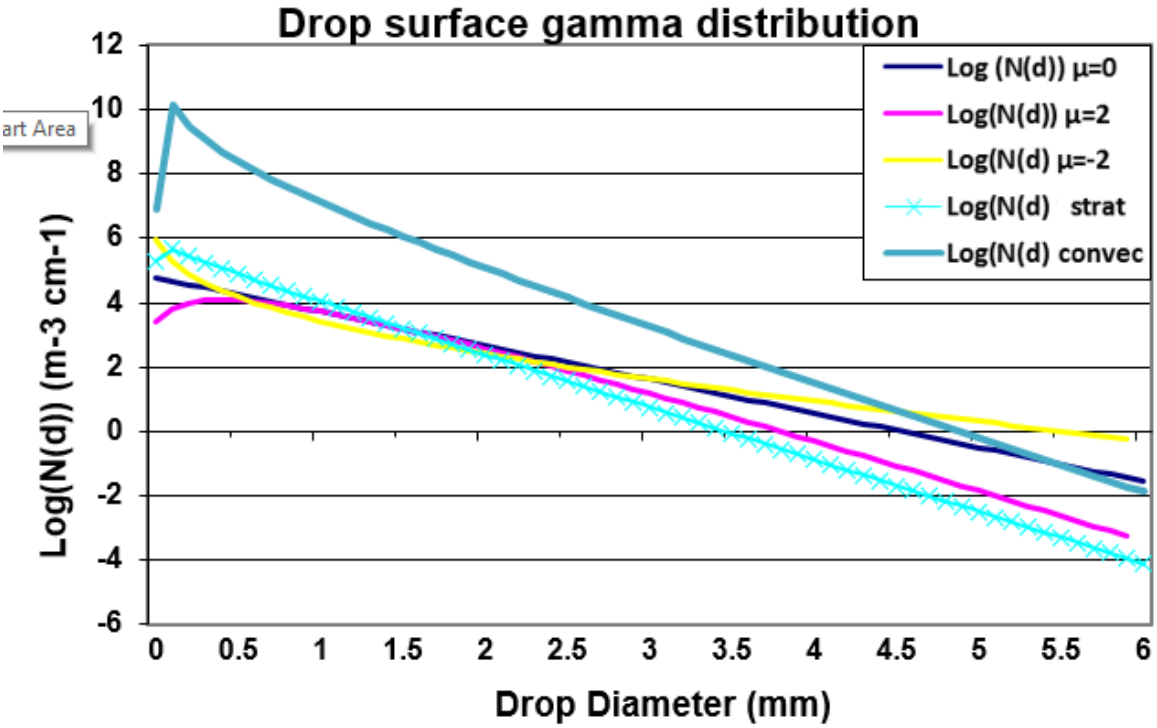

Figure 4. Gamma function of the drop size distribution for different μ values.

This number of drops is randomly assigned between the diameter values in the considered band. For each drop, the terminal and global velocities are determined (sum of the terminal and that due to the wind). This step also assigns the position of the space occupied by each of these drops at the initial time. With this information, it is possible to obtain the moments where the drop is in contact with the sensitive volume, which enables one to check whether at a given time, there are simultaneously several drops within the sensitive volume, and whether they can appear overlapping.

From these data, the rain signal is generated and repeated as many times as the number of trials to simulate. In our case, we worked with 20 or 200 simulations depending on the case.

At this point, the simulation of the behavior of the disdrometer is ready to begin. For this purpose, sampling period T is divided into subperiods of ΔT_{sam}; for each of these instants, the area covered by the drops in the sensitive volume is determined. Therefore, for each drop, we determine whether it is in contact, totally or partially, with the sensitive volume.

If the drop is completely inside the sensitive volume, the surface covered by the drop corresponds to the circle that represents its straight section

$$S = \pi\left(\frac{d}{2}\right)^2 \tag{9}$$

If the drop passes while rubbing the surface or only partially penetrates it, as shown in Figure 5, the covered surface S_T is

$$S_T = 2\left[R^2\left[\frac{\pi}{2} - \sin^{-1}\left(\frac{x_i}{R}\right) + \frac{x_i}{R}\sqrt{1-\left(\frac{x_i}{R}\right)^2}\right] + r^2\left[\frac{\pi}{2} + \sin^{-1}\left(\frac{x_i-b}{r}\right) - \frac{x_i-b}{r}\sqrt{1-\left(\frac{x_i-b}{R}\right)^2}\right]\right] \tag{10}$$

where

$$x_i = \frac{R^2 + b^2 - r^2}{2b} \tag{11}$$

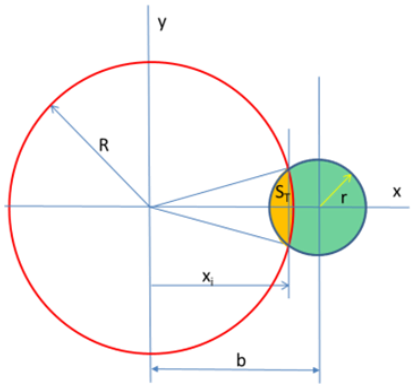

Figure 5. Representation of the surface covered by the passage of a drop through the sensitive volume.

From the measurements of the obstructed surface at each sampling instant and considering the resolution of the system, a series of discrete values is obtained for the drop size (function of the maximum surface obstructed) and duration of the signal. We assign each drop to any of the discrete drop sizes.

With this information, the filters to eliminate excessively large or small drops and temporary filters that enable one to eliminate the signals corresponding to splashes on the lenses are applied. Then, the corresponding corrections are applied to drops that pass while rubbing the sensitive volume. Finally, we can calculate the PI using the time and counting techniques.

3. Results

Figure 6 shows an example of the signals generated by the system for 1 s as a consequence of a stratiform rain of a precipitation intensity of 10 mm/h. From this general signal, a series of time intervals was extracted, where the signals that can induce errors in the estimation of the precipitation are appreciated. Thus, Figure 7 shows the case of a signal corresponding to a droplet that passes while rubbing the sensitive volume (A) and the case of a time interval where several drops simultaneously pass through the sensitive volume (B). Both types of signals will lead to errors in the precipitation estimation, and their effects must be corrected to make the measurement as accurate as possible.

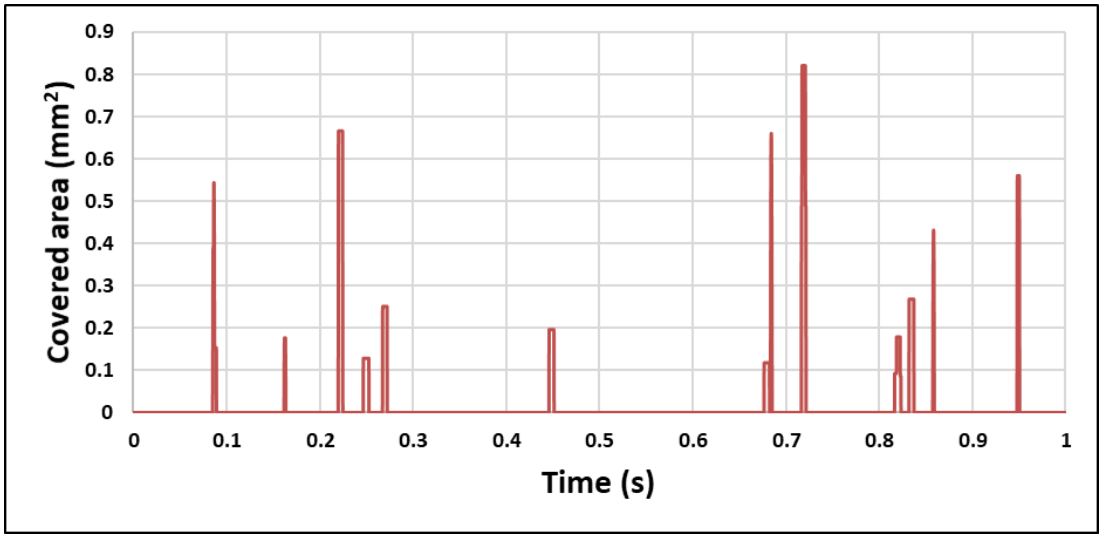

Figure 6. Signals generated by the passage of the droplets through the sensitive volume for 1 s with a precipitation intensity of 10 mm/h.

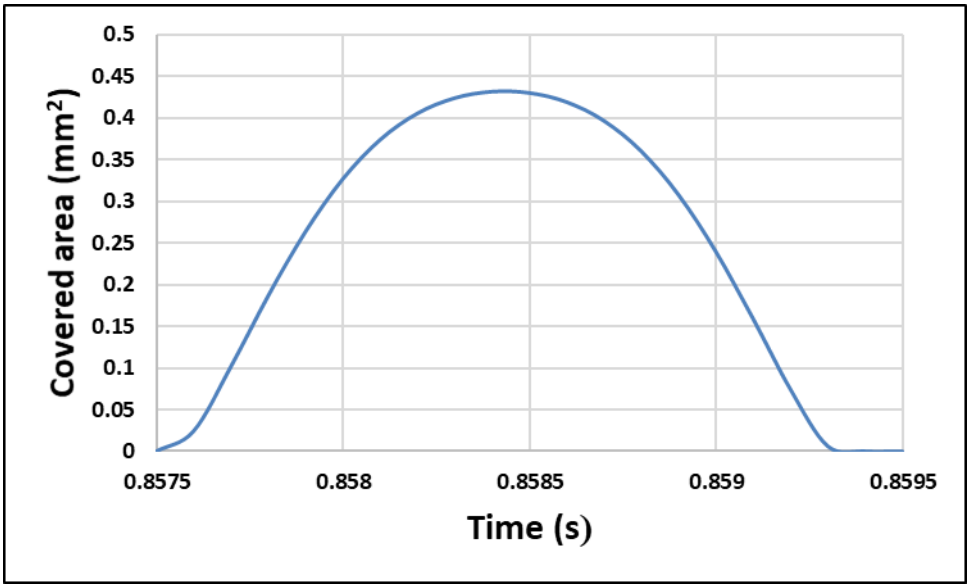

(**A**)

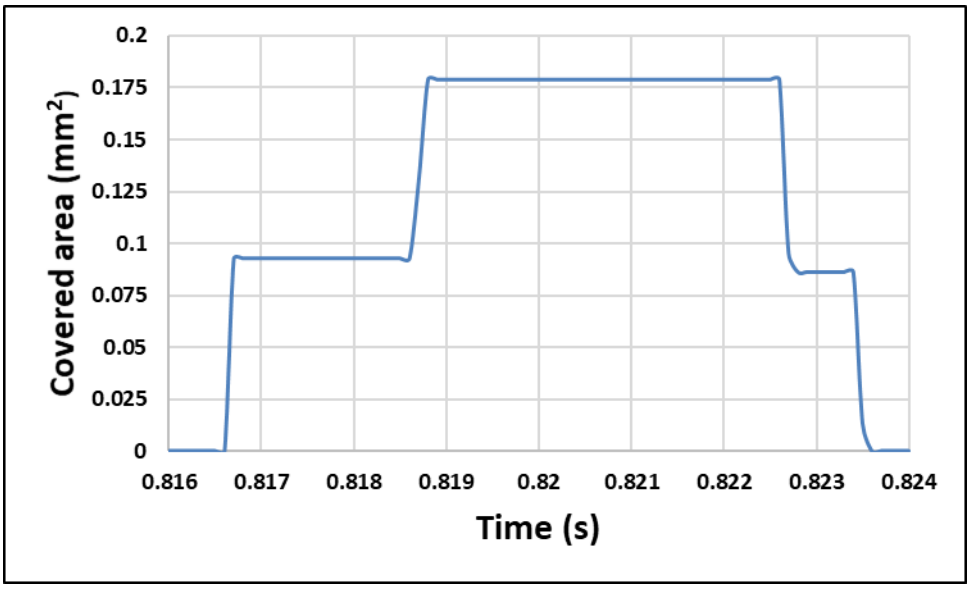

(**B**)

Figure 7. Superposition of several droplets simultaneously passing through the sensitive volume. (**A**) Signals generated by the passage; (**B**) A droplet that rubs the sensitive volume.

To determine the values that optimize the operation of the system, the following analyses were performed for different precipitation intensities (PIs):

1. The drop distribution was obtained according to their size: maintaining a constant number of drops of each size, we randomly generated different spatial and temporal distributions (200 analyses) to estimate the variations that could arise in the determination of the measured as a function of the position of the drops at the initial time.
2. The effect of considering different sampling times of 1−120 s was analyzed. To minimize the effect of the spatial and temporal distribution of the drops on the measurement, the average of 200 measurements with different distributions was analyzed.

3. The effect of the type of gamma distribution applied was analyzed by comparing the results of the stratiform and convective distribution.
4. The effect of the wind speed on the results of the counting and time estimation systems was analyzed. These measurements were performed for a PI of 5 mm/h with measurement periods of 5 s, resolution of 0.1 milliseconds and an average of 20 measurements.
5. The results were compared for 8- and 10-bit converters and an average of 20 measurements.

In this way, the main objective was to analyze the different aspects that can influence the quality of the readings offered by the optical disdrometers, such as the number of bits of the AD converters, sampling time, type of measurement technique, intensity of wind and precipitation. The results obtained from these analyses are shown in Figures 8–14, which represent:

1. The values of the precipitation measured with respect to the actual precipitation for different types of precipitation and measurement techniques (Figures 8 and 9).
2. Estimation of precipitation measurement error for different sampling times, measurement technique, and type of precipitation (Figure 10).
3. Estimate of the PI versus the real PI when working with 10-bit AD converters for different types of precipitation and measurement techniques (Figures 11 and 12).
4. Estimate of the IP versus the real IP when working with 8-bit AD converters for different types of precipitation and measurement techniques (Figures 13 and 14).

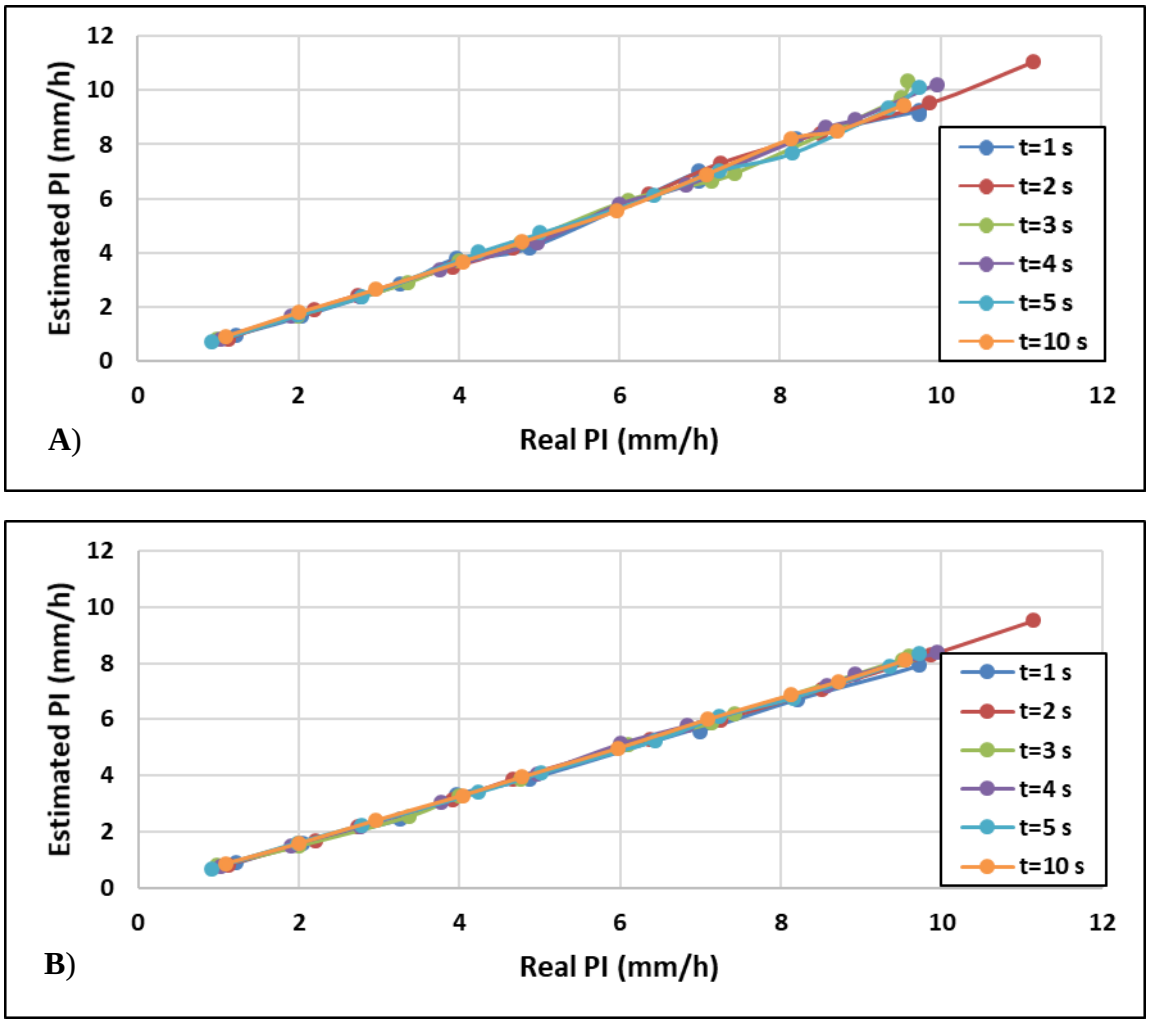

Figure 8. PI estimation for stratiform rainfall using the (**A**) time technique and (**B**) counting technique.

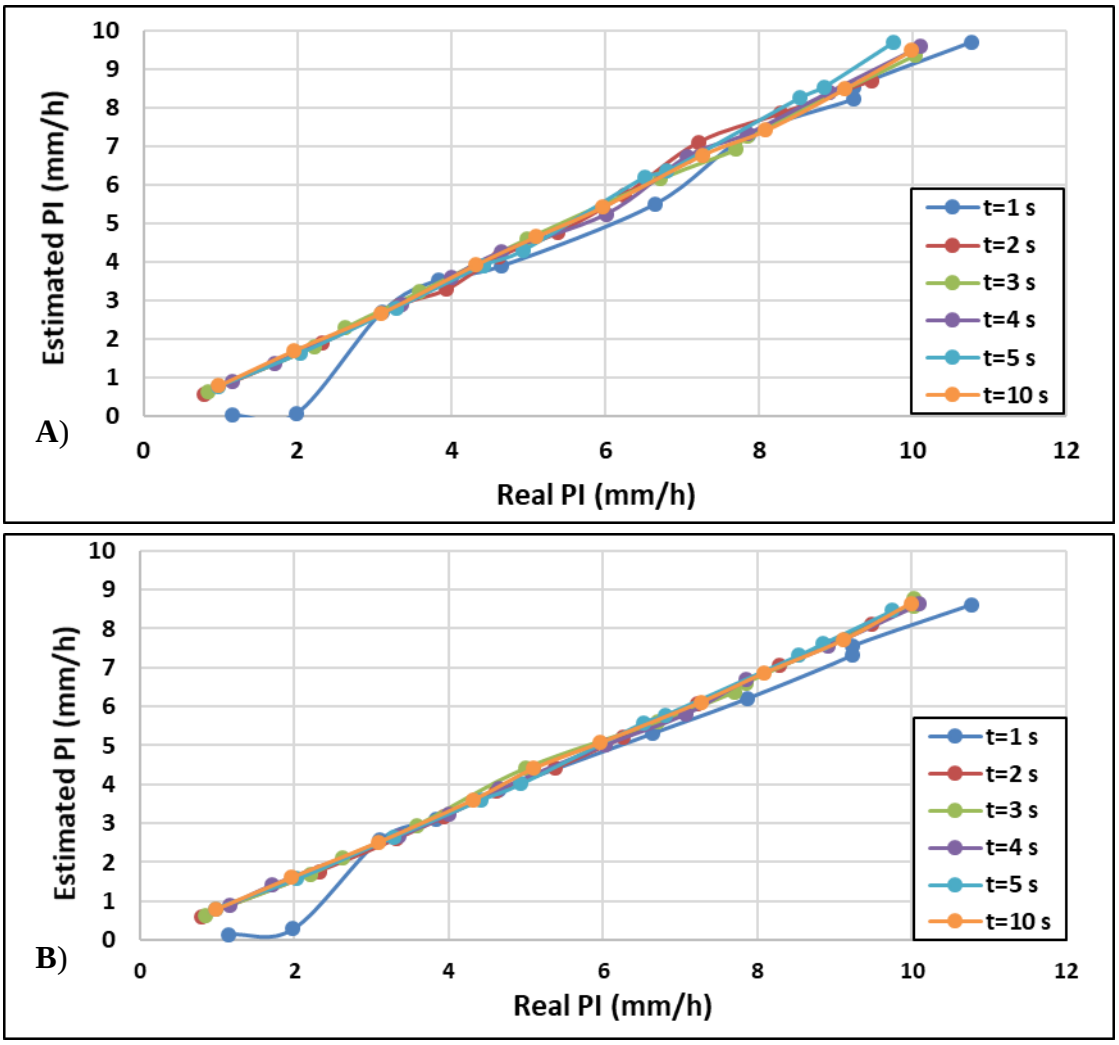

Figure 9. PI estimation for convective rainfall using the (**A**) time technique and (**B**) counting technique.

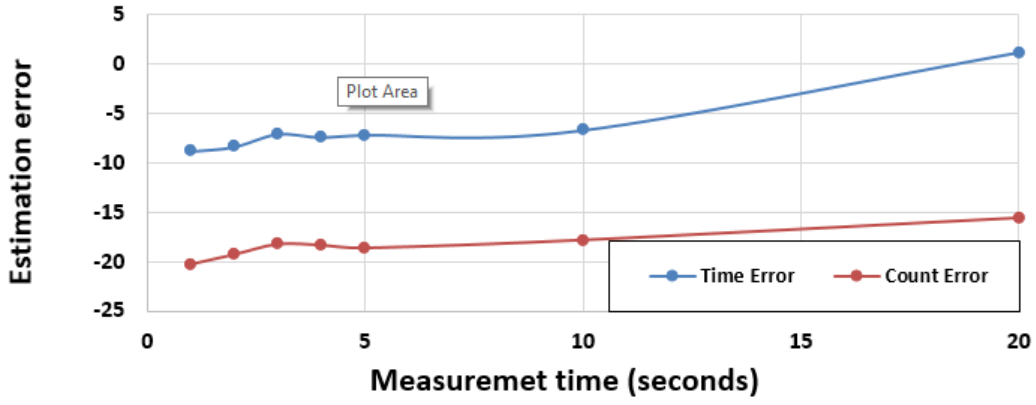

(**A**)

Figure 10. *Cont.*

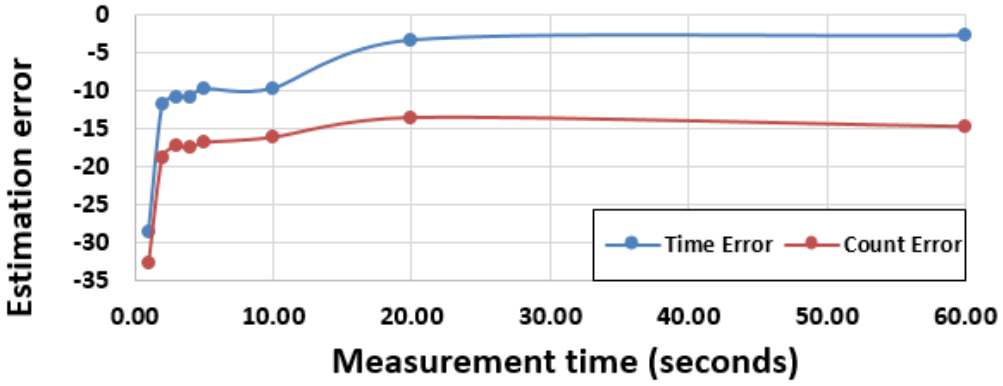

(**B**)

Figure 10. PI estimation errors of the counting and time techniques for different sampling times for (**A**) stratiform rain and (**B**) convective rain.

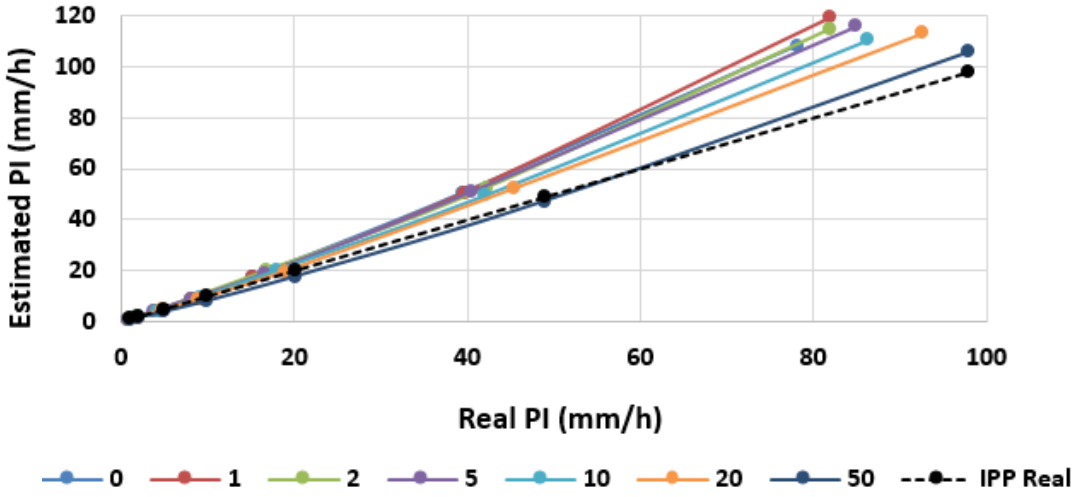

(**A**)

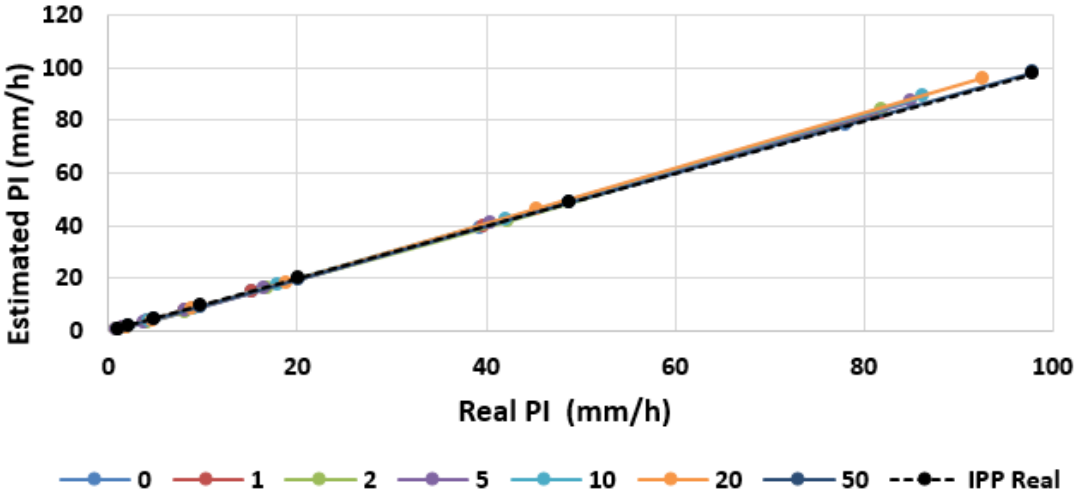

(**B**)

Figure 11. Estimated PI with 10-bit converters for stratiform rainfall, different precipitation intensities and different wind speeds: (**A**) time technique and (**B**) counting technique.

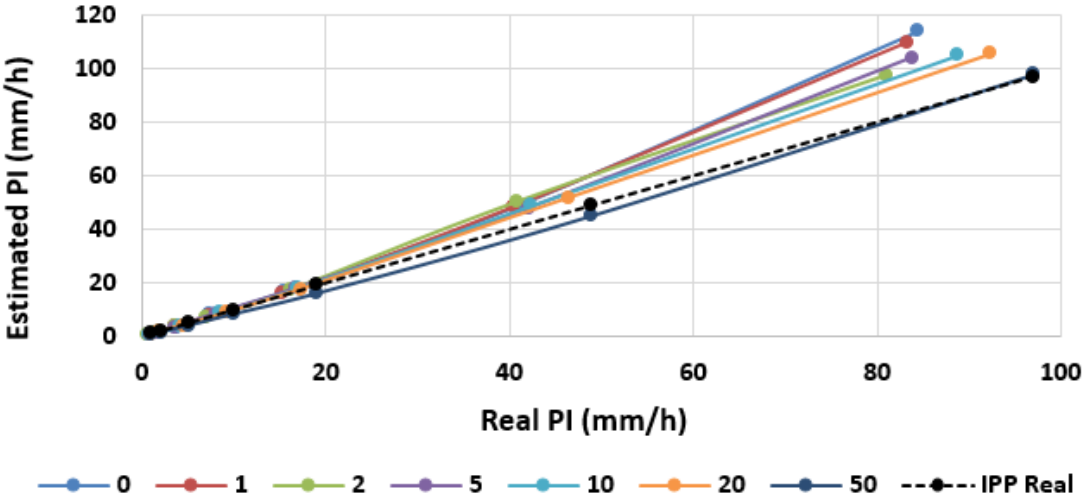

(**A**)

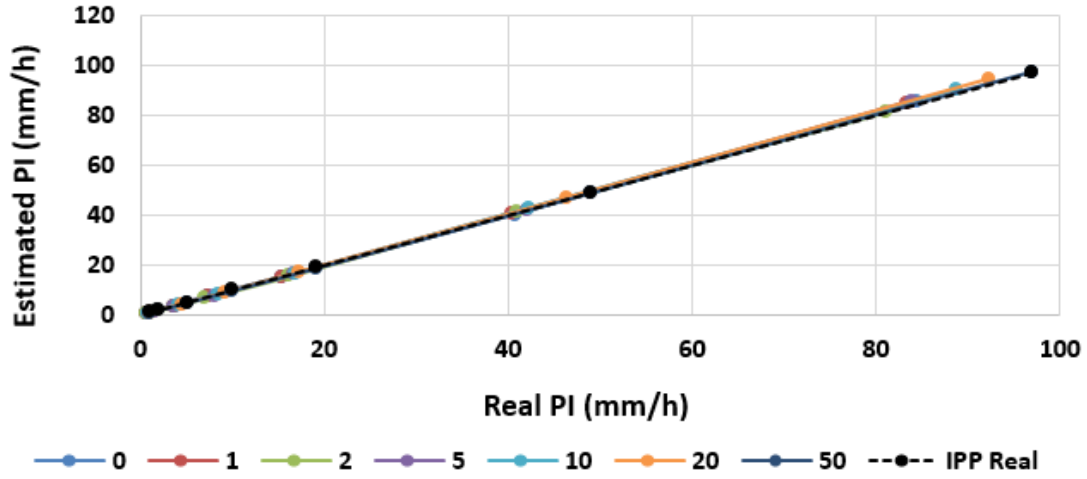

(**B**)

Figure 12. Estimated PI with 10-bit converters for convective rainfall, different precipitation intensities and different wind speeds: (**A**) time technique and (**B**) counting technique.

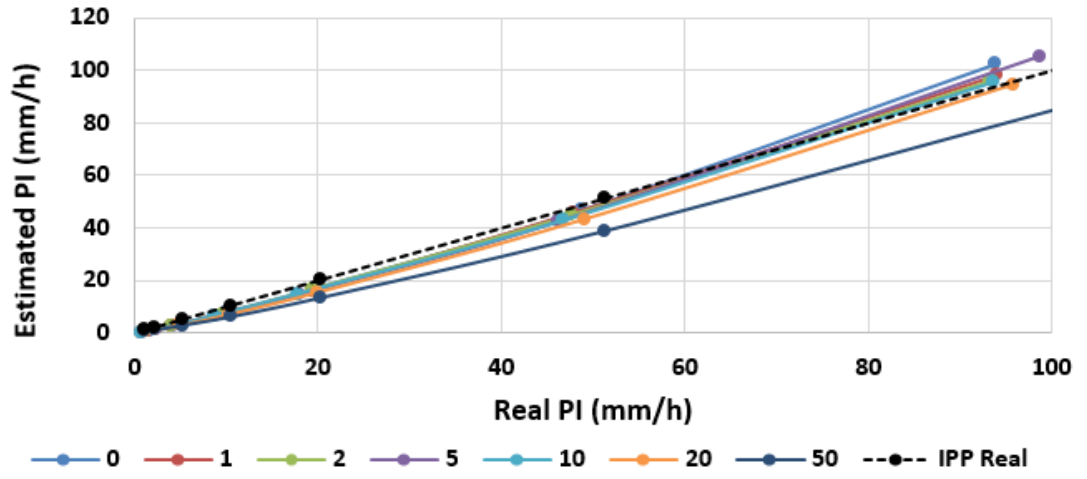

(**A**)

Figure 13. *Cont.*

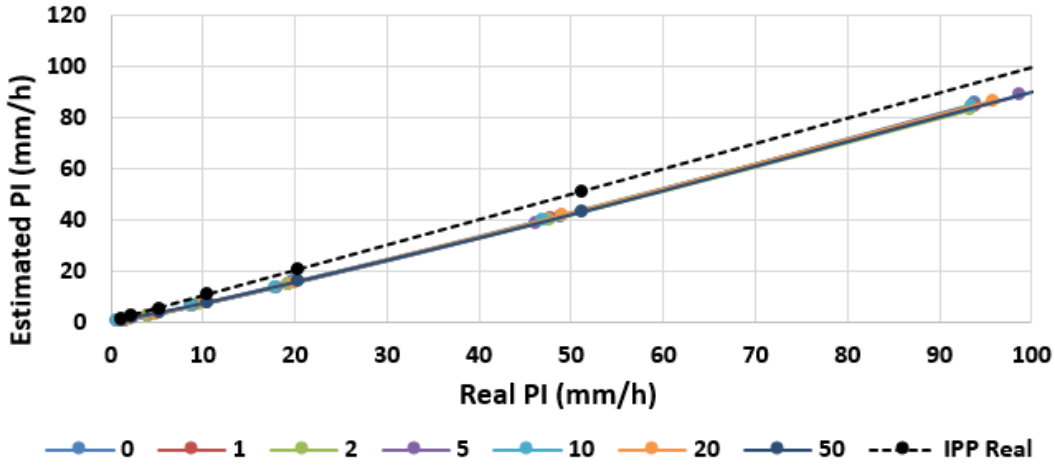

(**B**)

Figure 13. Estimated PI with 8-bit converters for stratiform rainfall, different precipitation intensities and different wind speeds: (**A**) time technique and (**B**) counting technique.

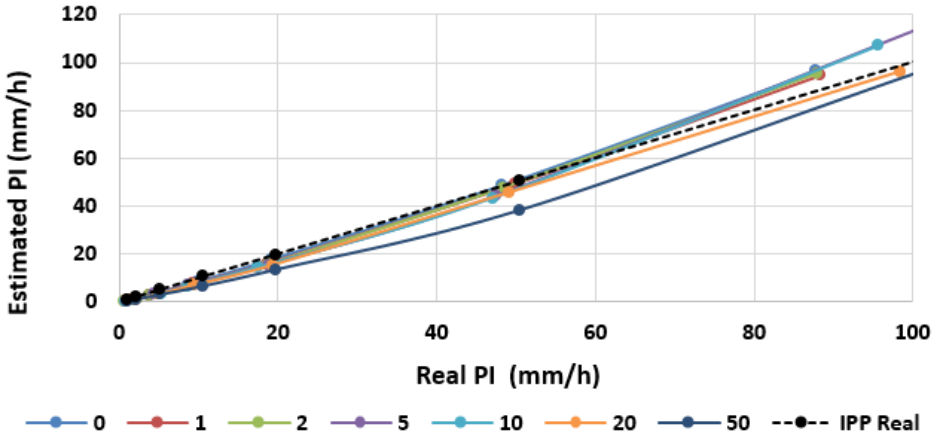

(**A**)

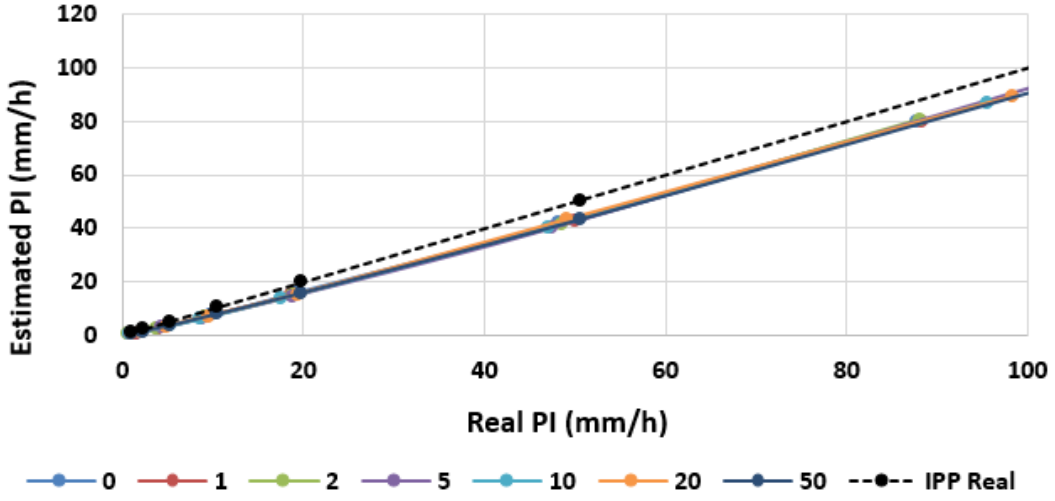

(**B**)

Figure 14. Estimated PI with 8-bit converters for convective rainfall, different precipitation intensities and different wind speeds: (**A**) time technique and (**B**) counting technique.

4. Discussion

Traffic accidents have an adverse effect both on an individual and societal level resulting in costs due to person injuries and property damage, increased travel times, and emissions due to congestion. Indeed, the safety impact of weather conditions has been actively studied in different studies [26–28], which conclude that accident risks are significantly heightened during rainy, snowy and icy road conditions. According to Salli et al. [29] the accident risk is more than four times higher for these conditions compared to bare road surface. However, a study based on data from the National Highway Traffic Safety Administration showed that rain and wet roads cause more car accidents and injuries than snow, sleet, or fog. Therefore, checking road conditions, especially rain, and properly warning users of it could help reduce the risk of landslides, collisions, or other unwanted traffic accidents.

Today, multiple options allow for quickly checking whether storms will slow down travel or keep the wheels running safely and smoothly. Sophisticated levels of information help time a drive and warn of pending weather-related dangers, learn whether an umbrella would be handy to bring along, or if a snowstorm is brewing. New technologies have simplified the search for this type of information and now this can be consulted by anyone. However, despite the fact that disdrometers have been used for many years on roads around the world, their performance has not been optimized for these scenarios. Hence the interest of this paper.

Accordingly, this research has analyzed the different aspects that can influence the quality of the readings offered by the optical disdrometers (such as number of bits of the AD converters, sampling time, type of measurement technique, wind intensity, and precipitation), has conducted an in-depth analysis of their impact on results and has proposed what should be the optimal values to use in each case, which will help in the design and implementation of future optical dysdrometers. Thus, this study aims to be a guide for the new disdrometers to be installed, which will be able to obtain more precise and detailed information on the state of the roads. In this way, accident reduction, better traffic management, and better quality of information provided to users will be achieved.

With the indicated computer model, a set of numerical simulations has been performed, where adequate measures were taken to limit the effect of multiple occupancies of the sensitive volume, tangential incidences, and presence of drops in the sensitive volume in the initial and final instants of the sampling period.

In this way, under these conditions and considering the results, the following conclusions are extracted:

1. The use of the counting technique always results in an estimate of precipitation the time technique.
2. The time technique usually overestimates of the precipitation values, except for precipitation intensities above 50 mm/h.
3. The counting technique provides very close estimated PI values to the actual values, which are slightly below them.
4. The PI measurement with 8-bit A/D converters provides better results with the time technique than with the counting technique. The latter usually underestimates the PI.
5. The PI measurement with 10-bit A/D converters provides better results with the counting technique than with the time technique. In this case, the latter usually overestimates the PI values.
6. For measurements using the time technique, the results show that it is better to work with 8-bit A/D converters.
7. For measurements using the counting technique, the results show that it is better to work with 10-bit A/D converters.
8. The edge effects have a smaller influence on the convective precipitation. The reason is that for a given precipitation intensity, the numerical density in the convective rain is less than that in the stratiform rainfall, and multiple occupations are less frequent.

In the counting technique, the effect of the wind on the PI estimation is practically negligible. In the time technique, there is a decrease in the PI estimation when the wind speed increases.

In conclusion, with the results of this study, the design and operation of the optical disdrometers could be optimized by knowing at any time, depending on the type of precipitation and the wind, which should be the type of estimation and the number of bits of the AD converter to be used. In addition, an estimate of the error made is also provided, which enables its correction. In this way, the results will allow to assess the convenience of using this type of system in ITS environments, which is our field of work. However, knowing these data, its configuration can also be optimized for other scenarios. Consequently, its application in urban and interurban environments would help to have more accurate information in real time, which would make it easier for management centers to apply the corresponding measures when there are adverse meteorological phenomena. These would result in an improvement of the information provided to users and therefore, in an increase in road safety and a decrease in the number of accidents due to these causes.

Author Contributions: Conceptualization, F.M.B., A.M.-M., and A.M.S.; Methodology, F.M.B., A.M.-M., and A.M.S.; Software, F.M.B., A.M.-M., and A.M.S.; Validation, F.M.B., A.M.-M., A.M.S., V.M.S., and M.J.P.A.; Formal analysis, F.M.B., A.M.-M., and A.M.S.; Investigation, F.M.B., A.M.-M., and A.M.S.; Resources, F.M.B., A.M.-M., and A.M.S.; Data curation, F.M.B., A.M.-M., and A.M.S.; Writing—original draft preparation, F.M.B.; Writing—review and editing, F.M.B.; Visualization, F.M.B. and M.J.P.A.; Supervision, F.M.B.; Project administration, F.M.B.; Funding acquisition, A.M.S. All authors have read and agreed to the published version of the manuscript.

Funding: This research has been funded by the Universitat Politècnica de València through its internal project "Equipos de detección, regulación e información en el sector de los sistemas inteligentes de transporte (ITS). Nuevos modelos y ensayos de compatibilidad y verificación de funcionamiento", which has been carried out at the ITACA Institute.

Conflicts of Interest: The authors declare no conflict of interest.

References

1. Frasson, R.P.D.M.; da Cunha, L.K.; Krajewski, W.F. Assessment of the thies optical disdrometer performance. *Atmos. Res.* **2011**, *101*, 237–255. [CrossRef]
2. Krajewski, W.F.; Kruger, A.; Caracciolo, C.; Golé, P.; Barthes, L.; Creutin, J.D.; Delahaye, J.-Y.; Nikolopoulos, E.I.; Ogden, F.; Vinson, J.P. DEVEX-disdrometer evaluation experiment: Basic results and implications for hydrologic studies. *Adv. Water Resour.* **2006**, *29*, 311–325. [CrossRef]
3. Peng, Y.; Jiang, Y.; Lu, J.; Zou, Y. Examining the effect of adverse weather on road transportation using weather and traffic sensors. *PLoS ONE* **2018**, *13*, e0205409. [CrossRef]
4. Ibrahim, A.; Hall, F. *Effect of Adverse Weather Conditions on Speed-Flow-Occupancy Relationships*; Transportation Research Record, No. 1457, TRB; National Research Council: Washington, DC, USA, 1994.
5. Rakha, H.; Arafeh, M.; Park, S. Modeling inclement weather impacts on traffic stream behavior. *Int. J. Transp. Sci. Technol.* **2012**, *1*, 25–47. [CrossRef]
6. Cruse, R.; Flanagan, D.; Frankenberger, J.; Gelder, B.; Herzmann, D.; James, D.; Krajewski, W.; Kraszewski, M.; Laflen, J.; Opsomer, J.; et al. Daily estimates of rainfall, water runoff, and soil erosion in Iowa. *J. Soil Water Conserv.* **2006**, *61*, 191–199.
7. Malin, F.; Norros, I.; Innamaa, S. Accident risk of road and weather conditions on different road types. *Accid. Anal. Prev.* **2019**, *122*, 181–188. [CrossRef] [PubMed]
8. Lolli, S.; Di Girolamo, P.; Demoz, B.; Li, X.; Welton, E.J. Rain Evaporation Rate Estimates from Dual-Wavelength Lidar Measurements and Intercomparison against a Model Analytical Solution. *J. Atmos. Ocean. Technol.* **2017**, *34*, 829–839. [CrossRef]
9. World Meteorological Organization. *Guide to Meteorological Instruments and Methods of Observation. WMO-No. 8*; WMO: Geneva, Switzerland, 2014.
10. Grossklaus, M.; Uhlig, K.; Hasse, L. An Optical Disdrometer for Use in High Wind Speeds. *J. Atmos. Ocean. Technol.* **1998**, *15*, 1051–1059. [CrossRef]
11. Hauser, D.; Amayenc, P.; Nutten, B.; Waldteufel, P. A new optical instrument for simultaneous measurement of raindrop diameter and fall speed distributions. *J. Atmos. Ocean. Technol.* **1984**, *1*, 256–269. [CrossRef]
12. Kathiravelu, G.; Lucke, T.; Nichols, P. Rain drop measurement techniques: A review. *Water* **2016**, *8*, 29. [CrossRef]

13. Illingworth, A.J.; Stevens, C.J. An optical disdrometer for the measurement of raindrop size spectra in windy conditions. *J. Atmos. Ocean. Technol.* **1987**, *4*, 411–421. [CrossRef]
14. Atlas, D.; Ulbrich, C.W. Path- and area-integrated rainfall measurement by microwave attenuation in the 1–3 cm band. *J. Appl. Meteorol.* **1977**, *16*, 1322–1331. [CrossRef]
15. Foote, G.B.; Torr, P.S.D. How fast do raindrops fall? Weather Guys Editor. Terminal Velocity of Raindrops Aloft. *J. Appl. Meteorol.* **2013**, *8*, 249–253. [CrossRef]
16. Pruppacher, H.R.; Pitter, R.L. A semi-empirical determination of the shape of cloud and rain drops. *J. Atmos. Sci.* **1971**, *28*, 86–94. [CrossRef]
17. Hasse, L.; Grossklaus, M.; Uhlig, K. *Measurement of Precipitation at Sea, Precipitation Measurement and Quality Control*; Institut für Meereskunde: Kiel, Slovakia, 1993.
18. Hasse, L.; Grossklaus, M.; Isemer, H.J.; Uhlig, K. *New Ship Rain Gage. Instruments and Observing Methods*; Report No 57. WMO/TD No 588; World Meteorological Organisation: Geneva, Switzerland, 1998; pp. 97–101.
19. Hasse, L.; Grossklaus, M.; Uhlig, K.; Timm, P. A ship rain gauge for use in high wind speeds. *J. Atmos. Ocean. Technol.* **1998**, *15*, 380–386. [CrossRef]
20. Marshall, J.S.; Palmer, W.M.K. The distribution of raindrops with size. *J. Meteorol.* **1948**, *5*, 165–166. [CrossRef]
21. Ulbrich, C.W. Natural variations in the analytical form of the raindrop size distribution. *J. Clim. Appl. Meteorol.* **1983**, *22*, 1764–1775. [CrossRef]
22. Ulbrich, C.W. The effects of drop size distribution truncation on rainfall integral parameters and empirical relations. *J. Clim. Appl. Meteorol.* **1985**, *24*, 580–590. [CrossRef]
23. Gertzman, H.S.; Atlas, D. Sampling errors in the measurement of rain and hail parameters. *J. Geophys. Res.* **1977**, *82*, 4955–4966. [CrossRef]
24. Brawn, D.; Upton, G. Estimation of an atmospheric gamma drop size distribution using disdrometer data. *Atmos. Res.* **2008**, *87*, 66–79. [CrossRef]
25. Zhang, G.; Vivekanandan, J.; Brandes, E.A.; Meneghini, R.; Kozu, T. The shape–slope relation in observed gamma raindrop size distributions: Statistical error or useful information? *J. Atmos. Ocean. Technol.* **2003**, *20*, 1106–1119. [CrossRef]
26. Peng, Y.; Abdel-Aty, M.; Lee, J.; Zou, Y. Analysis of the impact of fog-related reduced visibility on traffic parameters. *J. Transp. Eng.* **2018**, *144*, 04017077. [CrossRef]
27. Alves de Souza, B.; da Silva Rocha Paz, I.; Ichiba, A.; Willinger, B.; Gires, A.; Amorim, J.C.C.; de Miranda Reis, M.; Tisserand, B.; Tchiguirinskaia, I.; Schertzer, D. Multi-hydro hydrological modelling of a complex peri-urban catchment with storage basins comparing C-band and X-band radar rainfall data. *Hydrol. Sci. J.* **2018**, *63*, 1619–1635. [CrossRef]
28. Tabary, P.; Boumahmoud, A.-A.; Andrieu, H.; Thompson, R.J.; Illingworth, A.J.; Le Bouar, E.; Testud, J. Evaluation of two "integrated" polarimetric Quantitative Precipitation Estimation (QPE) algorithms at C-band. *J. Hydrol.* **2011**, *405*, 248–260. [CrossRef]
29. Salli, R.; Lintusaari, M.; Tiikkaja, H.; Pöllänen, M. *Keliolosuhteet ja Henkilöautoliikenteen Riskit [Wintertime Road Conditions and Accident Risks in Passenger Car Traffic]*; Tampere University of Technology, Department of Business Information Management and Logistics: Tampere, Finland, 2008.